

# 5-Aminoorotic acid, a versatile ligand with the ability to exhibit differing co-ordination and hydrogen-bonding modes: synthesis and crystal structures of platinum(II) complexes

Andrew D. Burrows,<sup>a,b</sup> D. Michael P. Mingos,<sup>a</sup> Andrew J. P. White<sup>a</sup> and David J. Williams<sup>a</sup>

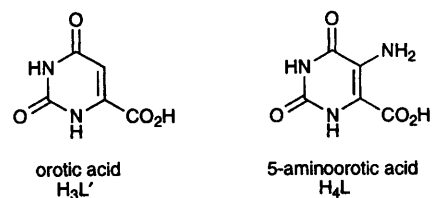
<sup>a</sup> Department of Chemistry, Imperial College of Science, Technology and Medicine, South Kensington, London SW7 2AY, UK

<sup>b</sup> School of Chemistry, University of Bath, Claverton Down, Bath BA2 7AY, UK

The complex  $[\text{Pt}(\text{cod})\text{Cl}_2]$  (cod = cycloocta-1,5-diene,  $\text{C}_8\text{H}_{12}$ ) reacted with 2 equivalents of  $\text{PPh}_3$  and an excess of 5-aminoorotic acid (5-amino-2,6-dioxo-1,2,3,6-tetrahydropyrimidine-4-carboxylic acid,  $\text{H}_4\text{L}$ ) in the presence of silver(I) oxide to give two isomers of  $[\text{Pt}(\text{PPh}_3)_2(\text{H}_2\text{L})]$  **1** and **2**. Complexes **1** and **2** can be separated by fractional crystallisation but, in  $\text{CDCl}_3$  solution, each slowly converts into an equilibrium mixture of the two. Crystal structure determinations have shown that in both **1** and **2** the 5-aminoorotate ligand co-ordinates to the platinum atom as a dianion. In **1** this is achieved *via* deprotonation of the carboxylic acid and the loss of an amino  $\text{NH}_2$  proton, leading to a six-membered chelate ring, whereas in **2** it is by deprotonation of the carboxylic acid and loss of the amido proton, leading to a five-membered chelate ring. This difference in co-ordination mode leads to a difference in the orientation of the hydrogen-bond donors and acceptors remaining on the ligand which, in turn, leads to different supramolecular structures, dimers for **1** and tetramers for **2**, with the latter structurally similar to guanine tetrads. These naturally occurring units are stabilised by alkali-metal ions, but reaction of **2** with a compound such as  $\text{NaBF}_4$  in a two-phase dichloromethane–water system led to  $[\text{Pt}_2(\text{PPh}_3)_4(\text{HL})][\text{BF}_4]$  as the only platinum-containing product. A crystal structure determination showed that in this complex the ligand is trianionic, deprotonated at the carboxylic acid and both the amido and amino nitrogen atoms, co-ordinating to two platinum atoms *via* five- and six-membered chelate rings. When dppe [1,2-bis(diphenylphosphino)ethane] was used instead of  $\text{PPh}_3$  only one isomer of  $[\text{M}(\text{dppe})(\text{H}_2\text{L})]$  ( $\text{M} = \text{Pt}$  or  $\text{Pd}$  **4**) was observed for both platinum and palladium, containing the five-membered chelate ring.

The incorporation of transition-metal ions into supramolecular aggregates with a view to exploiting their magnetic, optical and conductivity properties is attracting considerable interest.<sup>1,2</sup> Such aggregates may be prepared by taking advantage of the molecular recognition characteristics of multiple hydrogen-bond interactions.<sup>3–5</sup> We have previously shown that the derivatives of orotic acid (2,6-dioxo-1,2,3,6-tetrahydropyrimidine-4-carboxylic acid,  $\text{H}_3\text{L}'$ ),  $[\text{Pt}(\text{PR}_3)_2(\text{HL}')]_n$ , which contain a potential hydrogen-bond acceptor, hydrogen-bond donor, hydrogen-bond acceptor (ADA) array, are only able to utilise one donor and acceptor in the solid state forming double hydrogen bond-linked dimer pairs. More efficient use of the hydrogen-bonding sites can be made by cocrystallisation with a compound containing the complementary DAD arrangement of hydrogen-bonding sites such as 2,6-diaminopyridine.<sup>6</sup> There is a further interest in studying the platinum complexes of derivatives of naturally occurring nucleobases as they are involved in the antitumour activity of *cis*-platin  $[\text{Pt}(\text{NH}_3)_2\text{Cl}_2]$  and related compounds.<sup>7</sup> This has led to considerable development of the nucleobase chemistry of platinum amines,<sup>8</sup> though the chemistry of the phosphine derivatives has received less attention.<sup>9</sup>

Several complexes of 5-aminoorotic acid (5-amino-2,6-dioxo-1,2,3,6-tetrahydropyrimidine-4-carboxylic acid,  $\text{H}_4\text{L}$ ) with transition metals<sup>10,11</sup> or lanthanides<sup>12</sup> have been previously reported, though none has been characterised crystallographically. Here we report the synthesis, characterisation and crystal structures of three platinum(II) complexes of this ligand, each of which exhibits a different co-ordination mode. Two of the complexes, **1** and **2**, are isomeric forms of  $[\text{Pt}(\text{PPh}_3)_2(\text{H}_2\text{L})]$  in which the ligand has been doubly deprotonated, and binds to the metal through a six- or a five-

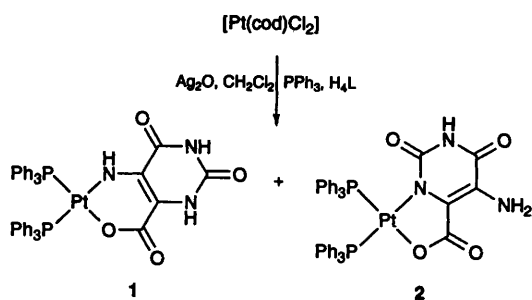


membered chelate ring. In the third complex, the ligand is triply deprotonated and binds to two metal atoms, one through the six-membered chelate ring observed in **1**, the other through the five-membered chelate ring in **2**. The co-ordination mode of the 5-aminoorotate ligand is shown to have a direct effect on the supramolecular structure adopted by the complex in the solid state and an interesting tetramer, reminiscent of those found in guanine tetrads, is observed for **2**.

## Results and Discussion

### Synthesis and characterisation of complexes $[\text{Pt}(\text{PPh}_3)_2(\text{H}_2\text{L})]$ **1** and **2**

The reaction of an excess of 5-aminoorotic acid with  $[\text{Pt}(\text{cod})\text{Cl}_2]$  (cod = cycloocta-1,5-diene,  $\text{C}_8\text{H}_{12}$ ), 2 equivalents of  $\text{PPh}_3$  and an excess of silver(I) oxide in refluxing dichloromethane gave two isomeric products, **1** and **2**, shown in Scheme 1, in similar yields. Complexes **1** and **2** were separated by fractional crystallisation from dichloromethane–hexane, with the lesser soluble isomer, **1**, crystallising first. The  $^{31}\text{P}\{^1\text{H}\}$  NMR data for **1** and **2** are summarised in Table 1. In both cases a pair of doublets with associated  $^{195}\text{Pt}$  satellites is



Scheme 1

Table 1 The  $^{31}\text{P}\{-^1\text{H}\}$  NMR data ( $\delta$ , J/Hz) for complexes 1–5

Compound	$\delta(\text{P}^1)^*$	$\delta(\text{P}^2)^*$	$^1J(\text{P}^1\text{Pt})$	$^1J(\text{P}^2\text{Pt})$	$^2J(\text{P}^1\text{P}^2)$
1	13.8	13.2	3021	3937	26
2	12.1	3.3	3445	3801	26
3	39.1	32.0	3294	3778	14
4	61.0	60.5	—	—	27
$5^+\text{BF}_4^-$	13.1	3.4	3399	3893	24
	11.8	11.8	3027	4050	24
$5^+\text{Cl}^-$	15.1	13.3	2960	3949	25
	8.0	15.3	3223	3969	19

\* In all cases  $\text{P}^1$  is defined as the phosphorus atom *trans* to nitrogen.

observed. Assignment of the signals is facilitated by the large difference in values of  $^1J(\text{PtP})$ , with the phosphorus *trans* to the carboxylate oxygen experiencing a larger coupling than the phosphorus *trans* to nitrogen. In contrast to the  $^{31}\text{P}\{-^1\text{H}\}$  NMR data, the  $^1\text{H}$  NMR spectra of 1 and 2 are diagnostic of the co-ordination modes, with  $^{195}\text{Pt}$  satellites observed only for the amino proton in 1. The spectrum of 1 in  $\text{CDCl}_3$  shows three resonances due to NH protons. The amido and imido protons give singlets at  $\delta_{\text{H}}$  8.02 and 7.95 and the amino proton gives a doublet of doublets at  $\delta_{\text{H}}$  4.27 [ $^3J(\text{HPt})$  4, 6 Hz] with  $^{195}\text{Pt}$  satellites [ $^2J(\text{HPt})$  68 Hz]. In the spectrum for 2 in  $\text{CDCl}_3$  the amino protons are observed at  $\delta_{\text{H}}$  5.45. The imido proton of 2 is not observed in  $\text{CDCl}_3$ , but is seen at  $\delta_{\text{H}}$  10.68 in  $(\text{CD}_3)_2\text{SO}$ .

The isomeric nature of complexes 1 and 2 is suggested by the FAB mass spectral data, with the two spectra being virtually identical. In both cases a peak at  $m/z$  888, corresponding to  $M^+$ , was observed as the highest-intensity peak, with smaller signals corresponding to  $\text{Pt}(\text{PPh}_3)_2^+$  ( $m/z$  719),  $\text{Pt}(\text{PPh}_3)^+$  ( $m/z$  457),  $\text{Pt}(\text{PPh}_2)^+$  ( $m/z$  380) and  $\text{Pt}(\text{PPh})^+$  ( $m/z$  303) also prominent.

The same two products, 1 and 2, can also be prepared from the reaction of  $[\text{Pt}(\text{PPh}_3)_2(\text{CO}_3)]$  with  $\text{H}_4\text{L}$  in dichloromethane. In this reaction the ratio of the two isomers is similar to that from the  $[\text{Pt}(\text{cod})\text{Cl}_2]$  reaction. This preparative route is less flexible, however, as a different carbonate starting material  $[\text{Pt}(\text{PR}_3)_2(\text{CO}_3)]$  would need to be prepared and isolated whenever a different phosphine is used. In contrast, the  $[\text{Pt}(\text{cod})\text{Cl}_2]$  reaction allows *cis*- $[\text{PtCl}_2(\text{PR}_3)_2]$  to be generated *in situ*.

In order to gain an insight into the exact nature of the isomerism, single-crystal X-ray analyses were undertaken on complexes 1 and 2. Suitable crystals were obtained for 1 from the slow diffusion of hexane into a solution of the complex in chloroform and for 2 the slow diffusion of hexane into a solution of the complex in dichloromethane. Selected bond lengths and angles for 1 and 2 are given in Tables 2 and 3 respectively. The crystal structure of 1 confirms that the aminoorotate is acting as a bidentate dianionic ligand following deprotonation at the carboxylic acid and amino groups, thus giving a six-membered chelate ring. The unit cell contains two crystallographically independent molecules, A and B, which are linked *via* two  $\text{N}-\text{H}\cdots\text{O}$  hydrogen bonds to form dimer pairs

Table 2 Selected bond lengths ( $\text{\AA}$ ) and angles ( $^\circ$ ) for complex 1

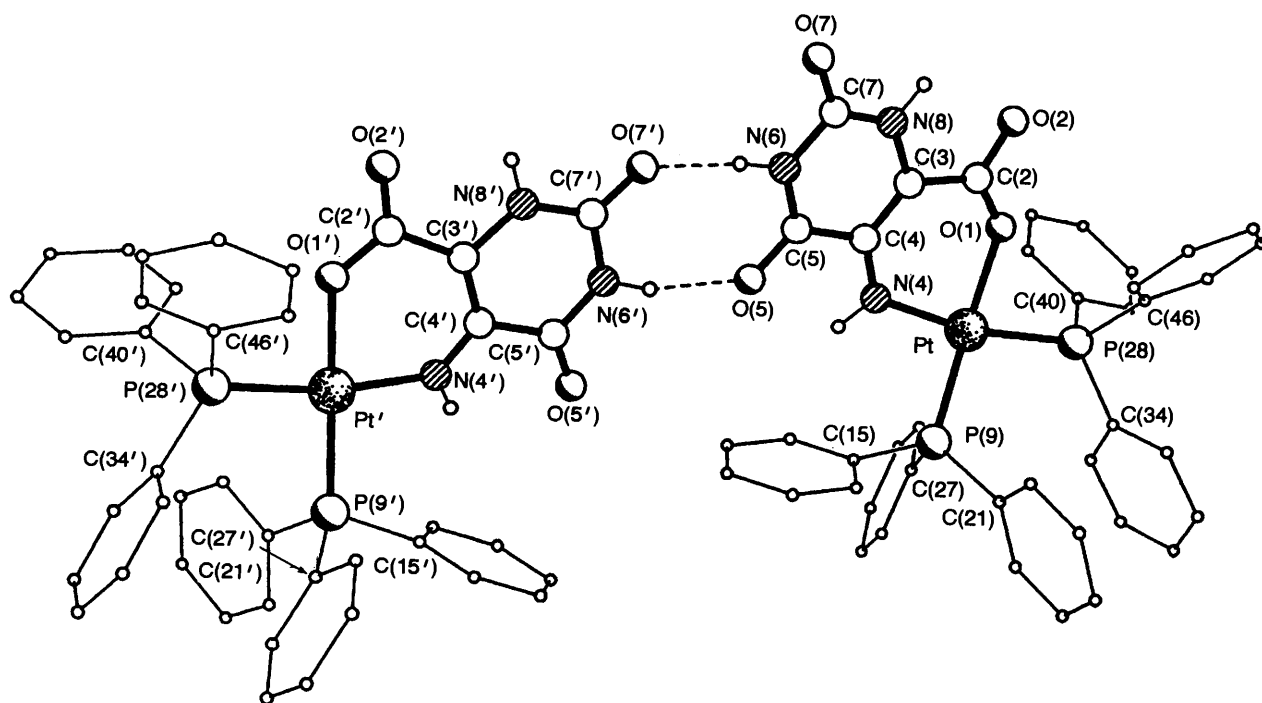
Pt–O(1)	2.072(13)	Pt–N(4)	2.005(15)
Pt–P(9)	2.240(5)	Pt–P(28)	2.297(5)
O(1)–C(2)	1.247(27)	C(2)–O(2)	1.251(28)
C(2)–C(3)	1.494(30)	C(3)–C(4)	1.338(27)
C(3)–N(8)	1.399(24)	C(4)–N(4)	1.311(25)
C(4)–C(5)	1.456(28)	C(5)–O(5)	1.285(27)
C(5)–N(6)	1.371(28)	N(6)–C(7)	1.379(28)
C(7)–O(7)	1.192(26)	C(7)–N(8)	1.300(28)
Pt'–O(1')	2.066(11)	Pt'–N(4')	2.043(14)
Pt'–P(9')	2.240(5)	Pt'–P(28')	2.291(5)
O(1')–C(2')	1.288(22)	C(2')–O(2')	1.215(24)
C(2')–C(3')	1.476(26)	C(3')–C(4')	1.388(28)
C(3')–N(8')	1.452(26)	C(4')–N(4')	1.250(24)
C(4')–C(5')	1.465(26)	C(5')–O(5')	1.180(26)
C(5')–N(6')	1.369(29)	N(6')–C(7')	1.406(31)
C(7')–O(7')	1.252(30)	C(7')–N(8')	1.317(29)
O(1)–Pt–N(4)	87.7(6)	O(1)–Pt–P(9)	177.3(5)
N(4)–Pt–P(9)	93.5(5)	O(1)–Pt–P(28)	80.7(4)
N(4)–Pt–P(28)	168.4(5)	P(9)–Pt–P(28)	98.1(2)
Pt–O(1)–C(2)	127.6(14)	O(1)–C(2)–O(2)	120.9(21)
O(1)–C(2)–C(3)	123.5(20)	O(2)–C(2)–C(3)	115.3(19)
C(2)–C(3)–C(4)	123.2(18)	C(2)–C(3)–N(8)	116.2(17)
C(4)–C(3)–N(8)	120.6(16)	C(3)–C(4)–N(4)	127.8(17)
C(3)–C(4)–C(5)	113.5(17)	N(4)–C(4)–C(5)	118.6(18)
Pt–N(4)–C(4)	126.1(13)	C(4)–C(5)–O(5)	118.8(19)
C(4)–C(5)–N(6)	120.7(19)	O(5)–C(5)–N(6)	120.2(18)
C(5)–N(6)–C(7)	124.3(17)	N(6)–C(7)–O(7)	118.5(20)
N(6)–C(7)–N(8)	111.7(19)	O(7)–C(7)–N(8)	129.5(20)
C(3)–N(8)–C(7)	128.6(17)	O(1')–Pt'–N(4')	86.5(5)
O(1')–Pt'–P(9')	180.0(6)	N(4')–Pt'–P(9')	93.5(5)
O(1')–Pt'–P(28')	83.2(3)	N(4')–Pt'–P(28')	169.7(4)
P(9')–Pt'–P(28')	96.7(2)	Pt'–O(1')–C(2')	131.0(12)
O(1')–C(2')–O(2')	123.3(17)	O(1')–C(2')–C(3')	117.3(17)
O(2')–C(2')–C(3')	119.3(18)	C(2')–C(3')–C(4')	128.2(18)
C(2')–C(3')–N(8')	112.6(17)	C(4')–C(3')–N(8')	119.1(16)
C(3')–C(4')–N(4')	124.6(17)	C(3')–C(4')–C(5')	118.5(18)
N(4')–C(4')–C(5')	116.6(17)	Pt'–N(4')–C(4')	128.1(13)
C(4')–C(5')–O(5')	123.6(20)	C(4')–C(5')–N(6')	115.1(18)
O(5')–C(5')–N(6')	121.1(18)	C(5')–N(6')–C(7')	128.7(17)
N(6')–C(7')–O(7')	123.7(20)	N(6')–C(7')–N(8')	113.7(20)
O(7')–C(7')–N(8')	122.5(22)	C(3')–N(8')–C(7')	124.7(18)

Table 3 Selected bond lengths ( $\text{\AA}$ ) and angles ( $^\circ$ ) for complex 2

Pt–O(1)	2.045(6)	Pt–N(8)	2.056(6)
Pt–P(9)	2.265(3)	Pt–P(28)	2.262(3)
O(1)–C(2)	1.317(11)	C(2)–O(2)	1.204(12)
C(2)–C(3)	1.493(11)	C(3)–C(4)	1.364(12)
C(3)–N(8)	1.392(10)	C(4)–N(4)	1.359(12)
C(4)–C(5)	1.448(12)	C(5)–O(5)	1.216(10)
C(5)–N(6)	1.353(11)	N(6)–C(7)	1.409(10)
C(7)–O(7)	1.235(10)	C(7)–N(8)	1.330(10)
O(1)–Pt–N(8)	79.3(2)	O(1)–Pt–P(9)	170.4(2)
N(8)–Pt–P(9)	96.6(2)	O(1)–Pt–P(28)	86.6(2)
N(8)–Pt–P(28)	165.9(2)	P(9)–Pt–P(28)	97.3(1)
Pt–O(1)–C(2)	117.0(5)	O(1)–C(2)–O(2)	122.7(8)
O(1)–C(2)–C(3)	114.3(8)	O(2)–C(2)–C(3)	122.9(8)
C(2)–C(3)–C(4)	121.7(8)	C(2)–C(3)–N(8)	114.7(7)
C(4)–C(3)–N(8)	123.4(7)	C(3)–C(4)–N(4)	125.4(8)
C(3)–C(4)–C(5)	118.3(8)	N(4)–C(4)–C(5)	116.2(8)
C(4)–C(5)–O(5)	125.2(8)	C(4)–C(5)–N(6)	114.4(7)
O(5)–C(5)–N(6)	120.3(7)	C(5)–N(6)–C(7)	127.2(7)
N(6)–C(7)–O(7)	118.5(7)	N(6)–C(7)–N(8)	116.2(7)
O(7)–C(7)–N(8)	125.3(7)	Pt–N(8)–C(3)	113.3(5)
Pt–N(8)–C(7)	126.7(5)	C(3)–N(8)–C(7)	119.9(7)

(Fig. 1). These hydrogen bonds involve the imido NH groups  $[\text{N}(6)$  and  $\text{N}(6')]$ † and the carbonyl oxygen atom adjacent to

† The crystallographic numbering scheme used in this paper differs from the standard numbering scheme of the ligand in order to retain consistency with and facilitate comparison to the orotate complexes reported previously.<sup>6</sup>



**Fig. 1** Molecular structure of the two independent molecules in complex **1** linked by two hydrogen bonds. The hydrogen-bond distances (Å) and angles (°) are N(6)···O(7') 2.78, H···O(7') 1.88, N(6)–H···O(7') 172 and N(6')···O(5) 2.88, H···O(5) 2.01, N(6')–H···O(5) 164

the amino group on one molecule [O(5)] and that adjacent to the amido NH group on the other molecule [O(7')] respectively.

The geometry at both platinum centres is slightly distorted square planar with angles in the ranges 80.7(4)–98.1(2) and 168.4(5)–177.3(5)° in A and 83.2(3)–96.7(2) and 169.7(4)–180.0(6)° in B. The O–Pt–N bond angles are, at 87.7(6) (A) and 86.5(5)° (B), as expected larger for the six-membered rings in **1** than for the five-membered rings in the related [Pt(dppe)(HL)].<sup>6</sup> Whereas the Pt–N [2.005(15) and 2.043(14) Å] and Pt–O [2.072(13) and 2.066(11) Å] distances are unexceptional, the Pt–P distances within each independent molecule differ markedly with those *trans* to nitrogen being significantly longer than those *trans* to oxygen [Pt–P(9) 2.240(5), Pt–P(28) 2.297(5); Pt'–P(9') 2.240(5), Pt'–P(28') 2.291(5) Å]. In both A and B there is a significant fold angle between the plane of the ligand and its platinum co-ordination plane [21° about the O(1)···N(4) and O(1')···N(4') vectors respectively]. Six-membered chelate rings based on 5-aminoorotic acid have also been proposed for copper and cobalt complexes,<sup>10</sup> though in these the ligand is believed to be monoanionic, being deprotonated only at the carboxylic acid.

The aminoorotate ligand, being well endowed with hydrogen-bond donors and acceptors, has the potential to adopt several modes of interligand hydrogen bonding. The asymmetric motif observed in the structure of complex **1** is not the pattern that one would have initially predicted: a symmetric arrangement involving a pair of *C<sub>s</sub>* symmetrically related molecules, using common donor and acceptor sites (and not requiring two crystallographically independent molecules), being more intuitive. Furthermore, the potential to form a more extended hydrogen-bonding network involving the other amino NH and carbonyl groups has also not been realised. An investigation into the packing of the molecules, and in particular the environments of the 'non-utilised' donor and acceptor sites, reveals (i) the presence of solvent domains (CHCl<sub>3</sub> molecules) proximal to O(2) and O(2') with chloroform CH groups lying within hydrogen-bonding distance of these carbonyl atoms,\* and (ii) that the regions close to O(7) and O(5') are occupied by phenyl rings from symmetrically related

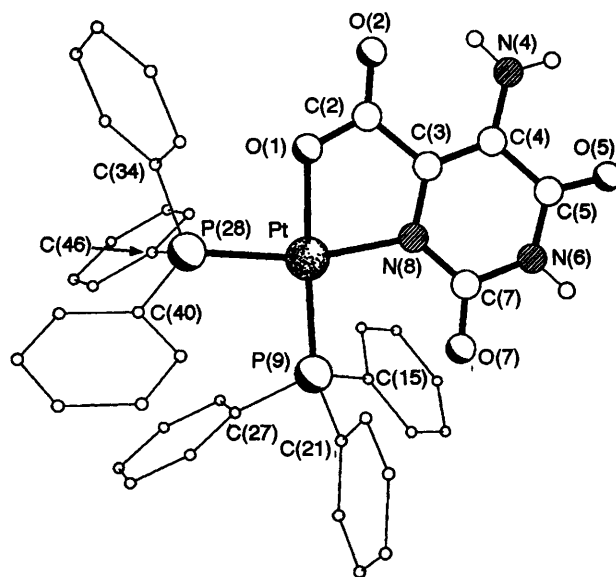


**Fig. 2** Molecular structure of complex **2**

molecules. It is thus reasonable to conclude that the 'asymmetric' hydrogen-bonding motif observed for **1** must to some extent be influenced by the presence of included solvent molecules capable of entering into hydrogen-bonding interactions.

The crystal structure of complex **2** demonstrates that the aminoorotate again acts as a bidentate dianionic ligand (Fig. 2), though in this case deprotonation has occurred at the carboxylic acid and *amido* groups, rather than the carboxylic acid and *amino* groups in **1**, giving a five-membered chelate ring, *cf.* the six-membered chelate ring of **1**. Thus the co-ordination

\* The detailed geometries of these potential hydrogen-bonding interactions are not discussed as they involve only partial-occupancy disordered solvent molecules.

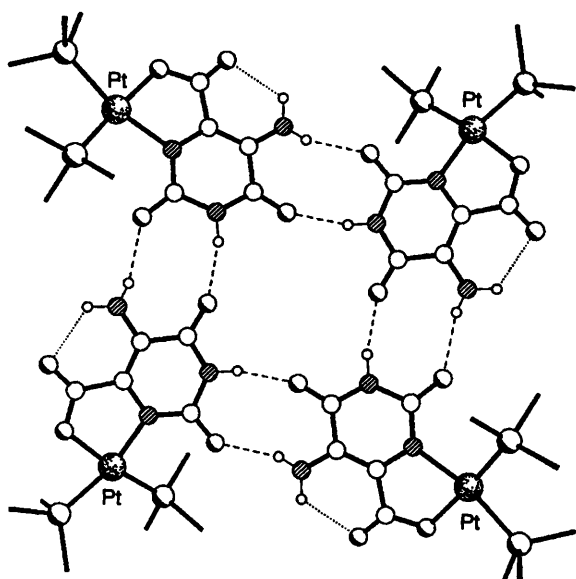


**Fig. 3** Hydrogen-bonded tetramers of complex **2**. The hydrogen-bond distances (Å) and angles (°) are N(6)⋯O(5) 2.85, H⋯O(5) 1.98 and N(6)–H⋯O(5) 163 for the inner imido NH-carbonyl linkage, N(4)⋯O(7) 2.87, H⋯O(7) 2.04 and N(4)–H⋯O(7) 152 for the outer amino NH-carbonyl linkage and N(4)⋯O(2) 2.73, H⋯O(2) 2.12 and N(4)–H⋯O(2) 124 for the intramolecular NH⋯O linkage

mode of the aminoorotate in **2** is directly analogous to that of orotate in [Pt(dppe)(HL')] with very similar bond lengths and angles.<sup>6</sup> The platinum co-ordination geometry is more distorted than that in **1**, with angles in the ranges 79.3(2)–97.3(1) and 165.9(2)–170.4(2)° and with a maximum deviation from planarity of 0.095 Å (*cf.* deviations of 0.032 and 0.009 Å for the two independent molecules in **1**). The Pt–O [2.045(6) Å] and Pt–N [2.056(6) Å] distances are very similar to those in **1**. Interestingly, however, the Pt–P distances, 2.265(3) Å to P(9) and 2.262(3) Å to P(28), are within statistical significance the same and do not reflect the presence of any *trans* influence. A similar effect is noted in solution, with the differences in the <sup>1</sup>J(PtP) coupling constants being 916 and 356 Hz for **1** and **2** respectively (Table 1). As in **1**, there is a significant deviation from coplanarity of the ligand and co-ordination planes, the pyrimidine ring being folded by *ca.* 17° out of the platinum co-ordination plane about the Pt–N(8) linkage.

The pattern of hydrogen bonding in complex **2** differs markedly from that in **1** with the molecules being linked *via* pairs of N–H⋯O hydrogen bonds between the imido N(6)–H atom and the pyrimidine carbonyl O(5) and between one of the amino N(4)–H atoms and the other pyrimidine carbonyl O(7) to form *S*<sub>4</sub> symmetric hydrogen-bonded tetramers (Fig. 3). This self-assembly of **2** into tetramers is reminiscent of naturally occurring guanine tetrads (or G quartets).<sup>13,14</sup> Such tetramers are stabilised in aqueous solution by alkali-metal ions and have been invoked in the structure of telomeric DNA<sup>15</sup> and other biological processes.<sup>16</sup> In these guanine tetrads the double hydrogen bonds linking the components have the two hydrogen bond donors on the Watson–Crick face and the two acceptors on the Hoogsteen face, hence the double hydrogen bonds can be represented as DD=AA. By contrast, in **2** the double hydrogen bonds have one donor and acceptor on each face, and consequently they can be represented as DA=AD. In the guanine tetrads the tetramers are stacked to form columns whereas in **2** this is prevented by the presence of the bulky Pt(PPh<sub>3</sub>)<sub>2</sub> groups. Complex **2** represents to our knowledge the first transition-metal complex to have this hydrogen-bonded tetrad structure. In addition, it appears to be the first tetrad structure to be based on pyrimidines as opposed to purines. There are a number of platinum tetramers known in which the metal atoms are linked through ligands bound by co-ordinative

bonds instead of hydrogen bonds. Bridging ligands that give rise to such tetramers include uracil,<sup>17</sup> 4,4'-bipyridine<sup>18</sup> and hydroxide.<sup>19</sup>

As in complex **1**, crystals of **2** contain chlorinated solvent molecules, though here there is only one partial-occupancy CH<sub>2</sub>Cl<sub>2</sub> molecule per metal complex. One of the hydrogen atoms of this solvent molecule lies within hydrogen-bonding distance of the carboxylic carbonyl oxygen atom O(2). In this instance, however, it appears to have no effect on the hydrogen-bonding network formed between aminoorotate ligands wherein all the hydrogen-bond donor and acceptor sites are utilised in either intra- or inter-ligand hydrogen-bonding interactions.

Although readily separated, both complexes **1** and **2** slowly isomerise in CDCl<sub>3</sub> or CH<sub>2</sub>Cl<sub>2</sub> to give an equilibrium mixture of the two isomers. The equilibrium constant, measured from the <sup>31</sup>P-{<sup>1</sup>H} NMR spectra, for the reaction **1** ⇌ **2** is 2.1(1). Equilibrium is reached after a period of several weeks, but the isomerisation appears to be catalysed by traces of acid present in the solvent. The rate of isomerisation is considerably reduced using freshly distilled solvent and no interconversion is observed using tetrahydrofuran (thf) as the solvent, even under reflux.

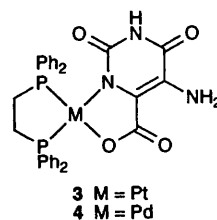
### Synthesis and characterisation of dppe complexes, **3** and **4**

Replacement of PPh<sub>3</sub> by dppe [1,2-bis(diphenylphosphino)ethane] led to significant differences in both the rate of reaction and the product distribution. With PPh<sub>3</sub>, complete conversion of the rapidly formed *cis*-[PtCl<sub>2</sub>(PPh<sub>3</sub>)<sub>2</sub>] into **1** and **2** was observed in less than 4 h. With dppe, however, some product was present after 4 h, although the major component in the reaction mixture was [PtCl<sub>2</sub>(dppe)], as identified from the <sup>31</sup>P-{<sup>1</sup>H} NMR spectrum. A reflux time of 24 h was required for all of this complex to react. In addition, only one product, **3**, was observed in the <sup>31</sup>P-{<sup>1</sup>H} NMR spectrum of the crude reaction product after 24 h. On the basis of <sup>1</sup>H NMR spectroscopy, **3** was characterised as containing a five-membered chelate ring, analogous to that in **2**.

Reaction of [PdCl<sub>2</sub>(dppe)] with H<sub>4</sub>L and silver(I) oxide also required 24 h reflux in CH<sub>2</sub>Cl<sub>2</sub> to reach completion. Again like the platinum analogue, only one product, **4**, was observed. It was also characterised as containing a five-membered chelate ring, analogous to that in **2**, on the basis of the <sup>1</sup>H NMR spectrum. The <sup>31</sup>P-{<sup>1</sup>H} NMR spectra of **3** and **4** showed no changes on standing for several weeks, suggesting that in contrast to the PPh<sub>3</sub> complexes no equilibria exist between the observed isomer and the potential isomer containing the bound amino nitrogen atom, analogous to **1**. Reaction of [Pd(cod)Cl<sub>2</sub>] with PPh<sub>3</sub>, H<sub>4</sub>L and Ag<sub>2</sub>O in an attempt to prepare palladium analogues of **1** and **2** was unsuccessful due to the rapid isomerisation of the initially formed *cis*-[PdCl<sub>2</sub>(PPh<sub>3</sub>)<sub>2</sub>] and precipitation of *trans*-[PdCl<sub>2</sub>(PPh<sub>3</sub>)<sub>2</sub>].

### Reactions of complexes **1** and **2** with alkali-metal ions

The similarity between the solid-state structure of complex **2** and the alkali metal-stabilised guanine tetrads led to the possibility that **2** might be able to act as a 'self-assembled crown ether'-like structure and co-ordinate Na<sup>+</sup> in the centre of the tetrad using the four inwardly directed oxygen lone pairs. Thus



an aqueous solution of  $\text{NaBF}_4$  was added to a dichloromethane solution of **2**, and the two-phase mixture was stirred vigorously for 10 h. The dichloromethane layer was then separated, the solvent evaporated, and the crude solid recrystallised from dichloromethane-hexane to give yellow crystals of  $5^+$  as its  $\text{BF}_4^-$  salt.

The IR spectrum confirmed the presence of the  $\text{BF}_4^-$  anion [ $\nu(\text{BF}_4)$  at  $1087\text{vs cm}^{-1}$ ] and showed small shifts in the values of  $\nu(\text{CO})$  and  $\nu(\text{NH})$ , consistent with co-ordination of  $\text{Na}^+$  to the tetramer. However, the  $^{31}\text{P}\{-^1\text{H}\}$  NMR spectrum showed the presence of four different phosphorus environments as opposed to the two expected for a tetrad-based structure. The spectrum, shown in Fig. 4, is deceptively simple due to the coincidence of two of the chemical shifts. These signals appear as a singlet, but have two associated sets of doublet  $^{195}\text{Pt}$  satellites. The spectrum has been successfully simulated, and the chemical shifts and coupling constants are given in Table 1. It is noticeable that these values for  $5^+\text{BF}_4^-$  are very similar to those for a combination of **1** and **2**, suggesting that *both* of the bidentate co-ordination sites on the ligand are occupied. The  $^{195}\text{Pt}$  NMR spectrum confirmed that there are two different platinum environments in  $5^+$ , with doublets of doublets observed at  $\delta -4054$  and  $-4143$ . Additional evidence for a complex containing two platinum atoms was obtained from the FAB mass spectrum, with peaks observed at  $m/z$  1607 ( $[M + \text{H}]^+$ , 100%) and 1694 ( $[M + \text{BF}_4]^+$ , 4%), assuming  $M$  is  $\text{Pt}_2(\text{PPh}_3)_4(\text{HL})$ .

In order to obtain more information on the structure of complex  $5^+\text{BF}_4^-$  a single-crystal X-ray analysis was undertaken. Suitable crystals were grown from the slow diffusion of hexane into a solution of the complex in dichloromethane. Selected bond lengths and angles are given in Table 4. The structure consists of discrete  $[\text{Pt}_2(\text{PPh}_3)_4(\text{HL})]^+$  cations and  $\text{BF}_4^-$  anions and the structure of the cation is shown in Fig. 5. The 5-aminoorotate acts as a trianionic ligand, being deprotonated at the carboxylic acid and at *both* the amino and amido nitrogen atoms. It is co-ordinated to two platinum atoms, one  $[\text{Pt}(47)]$  *via* a carboxylate oxygen and amino nitrogen, giving a six-membered chelate ring analogous to that in **1**, and the other  $[\text{Pt}(1)]$  *via* the second carboxylate oxygen and

the amido nitrogen, giving a five-membered chelate ring analogous to that in **2**.

The geometry at both platinum centres is slightly distorted square planar with angles in the range  $78.2(4)$ – $97.3(3)$  and  $164.1(3)$ – $173.9(2)$  at  $\text{Pt}(1)$  and  $81.5(2)$ – $98.1(1)$  and  $170.4(3)$ – $175.0(3)^\circ$  at  $\text{Pt}(47)$ . As expected the greater distortion is associated with the five-membered chelate ring, mirroring the greater distortion observed in complex **2** *cf.* **1**. As in both **1** and **2** there are significant deviations from planarity of the two platinum co-ordination planes with maximum deviations of  $0.086 \text{ \AA}$  for  $\text{Pt}(1)$  and  $0.064 \text{ \AA}$  for  $\text{Pt}(47)$ . The Pt–N, Pt–O and Pt–P distances are all very close to those observed in **1** [for  $\text{Pt}(47)$ ] and **2** [for  $\text{Pt}(1)$ ]. There are again folds of the co-ordination planes with respect to that of the ligand,  $10^\circ$  about  $\text{O}(2) \cdots \text{N}(4)$  for  $\text{Pt}(47)$  and  $28^\circ$  about  $\text{O}(1) \cdots \text{N}(8)$  for  $\text{Pt}(1)$ . In both **1** and **2** there are significant structural distortions in the ligand, necessary to accommodate either the five- or the six-membered chelate ring. This involves either an enlargement of the  $\text{C}(2)$ – $\text{C}(3)$ – $\text{C}(4)$  angle for the six-membered ring in **1** or a contraction of the  $\text{C}(2)$ – $\text{C}(3)$ – $\text{N}(8)$  angle for the five-membered ring in **2**. These are achieved simultaneously in complex  $5^+\text{BF}_4^-$  without any pyramidalisation at the  $\text{C}(3)$  centre (Table 4). As expected, there is a tendency towards equalisation of the two carboxylate C–O bond lengths in  $5^+$ .

The cations of complex  $5^+$  form hydrogen-bonded dimers linked by two  $\text{N-H} \cdots \text{O}$  hydrogen bonds involving the imino NH hydrogen atom and the adjacent carbonyl oxygen atom  $\text{O}(5)$  and *vice versa* of centrosymmetrically related pairs of molecules (Fig. 6). This observed hydrogen-bonding pattern represents one of three potential  $\text{DA}=\text{AD}$  motifs involving the imino NH group and its two neighbouring carbonyl oxygen atoms. It appears that the formation of the five-membered chelate ring *syn* to  $\text{O}(7)$  effectively blocks formation of  $\text{C}_i$  symmetrically related dimer pairs utilising  $\text{N}(6)$ – $\text{H}$  and  $\text{O}(7)$ .

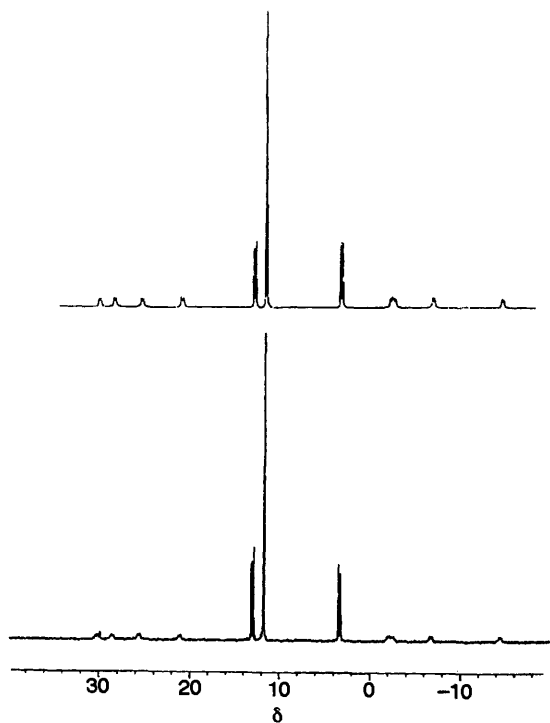


Fig. 4 Observed (below) and simulated (above)  $^{31}\text{P}\{-^1\text{H}\}$  NMR spectrum for complex **5**

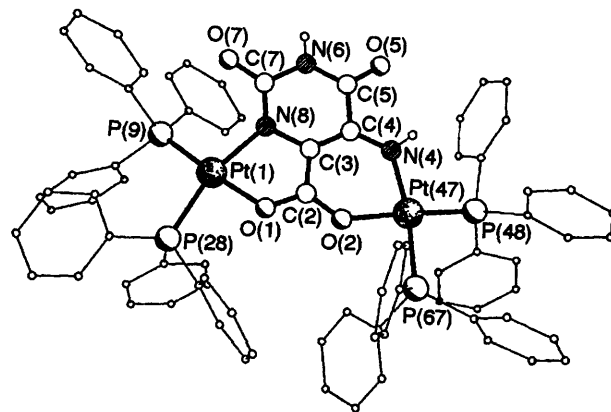


Fig. 5 Molecular structure of the cation of complex **5**

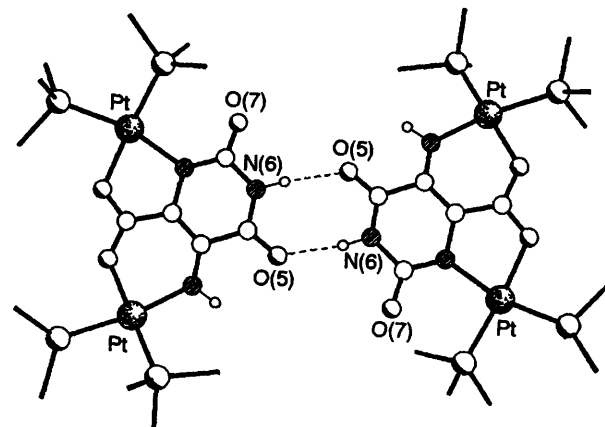


Fig. 6 Hydrogen-bonded dimers of complex  $5^+$ . The hydrogen-bond distances ( $\text{\AA}$ ) and angles ( $^\circ$ ) are  $\text{N}(6) \cdots \text{O}(5\text{A})$  2.89,  $\text{H} \cdots \text{O}(5\text{A})$  2.00 and  $\text{N}(6)\text{--H} \cdots \text{O}(5\text{A})$  173

**Table 4** Selected bond lengths (Å) and angles (°) for complex  $5^+BF_4^-$ 

Pt(1)–O(1)	2.055(8)	Pt(1)–N(8)	2.063(9)
Pt(1)–P(9)	2.248(4)	Pt(1)–P(28)	2.269(3)
O(1)–C(2)	1.267(13)	C(2)–O(2)	1.276(13)
C(2)–C(3)	1.43(2)	O(2)–Pt(47)	2.048(8)
C(3)–C(4)	1.35(2)	C(3)–N(8)	1.45(2)
C(4)–N(4)	1.31(2)	C(4)–C(5)	1.48(2)
N(4)–Pt(47)	1.991(10)	C(5)–O(5)	1.230(13)
C(5)–N(6)	1.33(2)	N(6)–C(7)	1.41(2)
C(7)–O(7)	1.24(2)	C(7)–N(8)	1.32(2)
Pt(47)–P(48)	2.236(3)	Pt(47)–P(67)	2.294(3)
O(1)–Pt(1)–N(8)	78.2(4)	O(1)–Pt(1)–P(9)	173.9(2)
N(8)–Pt(1)–P(9)	97.3(3)	O(1)–Pt(1)–P(28)	87.3(2)
N(8)–Pt(1)–P(28)	164.1(3)	P(9)–Pt(1)–P(28)	96.69(12)
C(2)–O(1)–Pt(1)	114.9(8)	O(1)–C(2)–O(2)	116.9(10)
O(1)–C(2)–C(3)	118.9(11)	O(2)–C(2)–C(3)	124.0(11)
C(2)–O(2)–Pt(47)	126.3(7)	C(4)–C(3)–C(2)	124.3(12)
C(4)–C(3)–N(8)	123.9(11)	C(2)–C(3)–N(8)	111.8(10)
N(4)–C(4)–C(3)	127.5(12)	N(4)–C(4)–C(5)	117.1(11)
C(3)–C(4)–C(5)	115.4(12)	C(4)–N(4)–Pt(47)	126.4(8)
O(5)–C(5)–N(6)	121.8(11)	O(5)–C(5)–C(4)	121.2(12)
N(6)–C(5)–C(4)	117.1(11)	C(5)–N(6)–C(7)	126.8(11)
O(7)–C(7)–N(8)	124.1(12)	O(7)–C(7)–N(6)	119.4(12)
N(8)–C(7)–N(6)	116.4(13)	C(7)–N(8)–C(3)	119.4(10)
C(7)–N(8)–Pt(1)	129.3(9)	C(3)–N(8)–Pt(1)	111.1(7)
N(4)–Pt(47)–O(2)	88.9(4)	N(4)–Pt(47)–P(48)	91.6(3)
O(2)–Pt(47)–P(48)	175.0(3)	N(4)–Pt(47)–P(67)	170.4(3)
O(2)–Pt(47)–P(67)	81.5(2)	P(48)–Pt(47)–P(67)	98.05(13)

An approach of N(6) and O(5) in one molecule to O(7) and N(6) in another, a geometry directly analogous to that observed in **1**, presents a less-hindered arrangement but is still more congested than the pattern actually observed involving N(6) and O(5) and their centrosymmetrically related counterparts. Although there is a degree of solvation in the crystals, neither these molecules nor the  $BF_4^-$  anions appear to influence the observed hydrogen-bonding pattern.

Complex **1** also reacts with  $NaBF_4$  under similar conditions to give  $5^+BF_4^-$  as the only platinum-containing product. The presence of water is not necessary for the conversion of either **1** or **2** into  $5^+$ . Complex  $5^+$  can also be prepared from **2** and  $NaBPh_4$  in dichloromethane–ethanol or even from  $NaBF_4$  in dichloromethane, though in this case the rate of the reaction is considerably reduced by the insolubility of  $NaBF_4$  in this solvent. The cation does not need to be  $Na^+$  and conversion of **2** into  $5^+$  as its  $BF_4^-$ ,  $PF_6^-$ ,  $NO_3^-$  or  $Cl^-$  salt has also been achieved with  $K^+$ ,  $Li^+$ ,  $Rb^+$ ,  $Cs^+$  and  $Zn^{2+}$ . It is noticeable that when the anion is nitrate the reaction occurs at a considerably slower rate than when it is  $BF_4^-$  or  $PF_6^-$ . A metal ion,  $M^+$  or  $M^{2+}$ , however, does appear to be needed to facilitate the reaction, perhaps to stabilise the  $H_3L^-$  by-product; no trace of  $5^+$  was observed after stirring **2** with  $NBu_4^+PF_6^-$  in dichloromethane for 10 h.

In the reaction with a metal chloride the  $^{31}P\text{-}\{^1H\}$  NMR spectrum was somewhat different from those obtained with other anions (Table 1). There are no longer two coincident chemical shifts, and four doublets with  $^{195}Pt$  satellites are observed. The spectroscopic and analytic data are, however, still consistent with the formulation of  $5^+$  as its  $Cl^-$  salt. Identical  $^{31}P\text{-}\{^1H\}$  NMR spectra were obtained on refluxing **1** in dichloromethane for 6 h. This reaction was expected to lead to the rapid equilibrium of **1** and **2**, but instead the  $Cl^-$  salt of  $5^+$  was the only product observed. In this reaction chloride is abstracted from the solvent and no reaction was observed on refluxing **1** with thf as the solvent.

In order to confirm that the product of these two reactions is the  $Cl^-$  salt of  $5^+$ , the compound was also prepared in a more rational manner. Since *cis*- $[PtCl_2(PPh_3)_2]$  has been shown to react with  $H_4L$  in the presence of  $Ag_2O$  to give **1** and **2**, it should also react with either **1** or **2**, each of which essentially contains

an unreacted ligand face, to give  $5^+$ . When complex **1** was refluxed in thf with *cis*- $[PtCl_2(PPh_3)_2]$  and  $Ag_2O$ , a yellow precipitate was produced, which was indeed identified on the basis of  $^{31}P\text{-}\{^1H\}$  NMR spectroscopy as the  $Cl^-$  salt of  $5^+$ . The reactions leading to the  $BF_4^-$  and  $Cl^-$  salts of  $5^+$  are summarised in Scheme 2.

## Conclusion

The results above clearly demonstrate the versatility of the 5-aminoorotate ligand, which adopts three co-ordination modes, involving either one or two platinum atoms. In addition to the structural characterisation, the presence of five- and six-membered chelate rings has been indicated by  $^1H$  NMR spectra, with  $^{195}Pt$  satellites from the  $^2J(HPt)$  coupling observed only in the latter. The choice of nitrogen donor atoms (amido or amino) leads to differences in the orientation of the hydrogen-bond donor and acceptor groups remaining on the ligand, and this has been shown to have a major effect on the supramolecular structures adopted by the complexes, with hydrogen-bonded dimers observed for **1** and  $5^+BF_4^-$ , but hydrogen-bonded tetramers, structurally similar to naturally occurring guanine tetrads, observed for **2**.

## Experimental

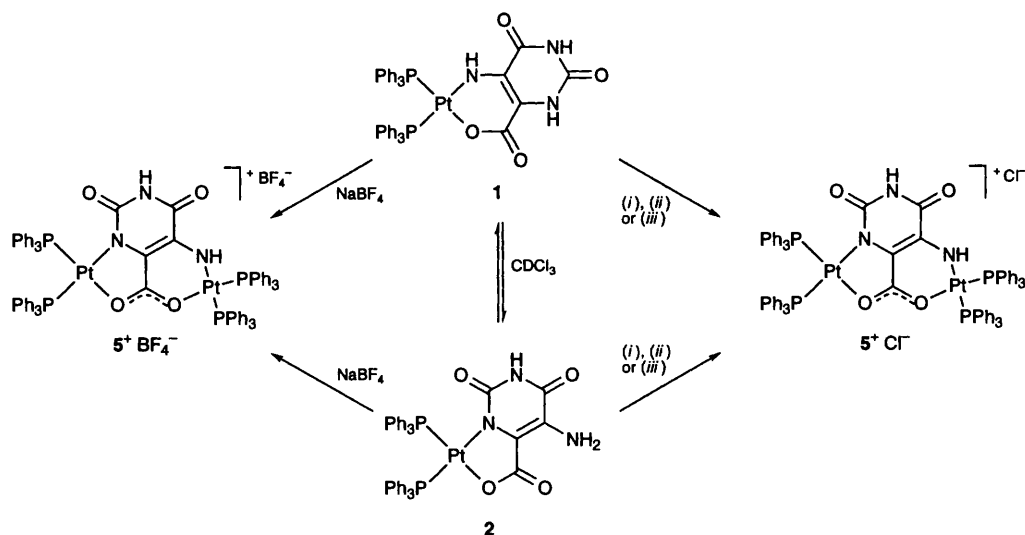
Reactions were routinely carried out using Schlenk-line techniques under pure dry dinitrogen using dioxygen-free solvents, but no special precautions were taken to exclude oxygen during work-up procedures. Microanalyses (C, H and N) were carried out by the Imperial College Microanalytical Service. Infrared spectra were recorded on a Perkin-Elmer 1720 spectrometer as KBr pellets,  $^1H$ ,  $^{31}P\text{-}\{^1H\}$  and  $^{195}Pt$  NMR spectra on a JEOL JNM-EX270 spectrometer operating at 270 MHz referenced to  $SiMe_4$ , 109.4 MHz referenced to  $H_3PO_4$  and 58.1 MHz referenced to  $Na_2PtCl_6$ , respectively. The FAB mass spectra were recorded on a VG AutoSpec-Q spectrometer using 3-nitrobenzyl alcohol as the matrix.

The complexes  $[Pt(cod)Cl_2]$ ,<sup>20</sup>  $[Pd(cod)Cl_2]$ <sup>21</sup> and  $[Pt(PPh_3)_2(CO_3)]$ <sup>22</sup> were prepared by the standard literature methods.

## Syntheses

**Isomers of  $[Pt(PPh_3)_2(H_2L)]$  **1** and **2**.** *Method 1.* Triphenylphosphine (0.420 g, 1.60 mmol) was added to a solution of  $[Pt(cod)Cl_2]$  (0.300 g, 0.80 mmol) in dichloromethane (30 cm<sup>3</sup>) to give a colourless solution of *cis*- $[PtCl_2(PPh_3)_2]$ . The compound  $H_4L$  (0.500 g, 2.92 mmol) and silver(I) oxide (0.640 g, 2.76 mmol) were added and the mixture was refluxed for 4 h. The resulting yellow solution was filtered to remove unreacted  $H_4L$  and  $Ag_2O$ , and the solvent removed under reduced pressure. The crude product was recrystallised from dichloromethane–hexane to give yellow crystals of complex **1** (0.345 g, 48%). These were separated by filtration, and further hexane was added to the filtrate to give yellow crystals of **2** (0.306 g, 43%). Complex **1** (Found: C, 51.0; H, 3.6; N, 4.2.  $C_{41}H_{33}N_3O_4P_2Pt \cdot 1.25CH_2Cl_2$  requires C, 51.0; H, 3.6; N, 4.2%):  $\tilde{\nu}_{max}/cm^{-1}(CO)$  1694s, 1624s and 1597s; (NH) 3460w (br), 3343s and 3165m;  $\delta_H(CDCl_3)$  8.02 (1 H, s, NH), 7.95 (1 H, s, NH), 7.7–7.1 (30 H, m, Ph) and 4.27 [1 H, dd,  $^2J(HPt)$  68,  $^3J(HP)$  4, 6 Hz, NH];  $m/z$  888 ( $M^+$ ). Complex **2** (Found: C, 52.7; H, 3.7; N, 4.5.  $C_{41}H_{33}N_3O_4P_2Pt \cdot 0.75CH_2Cl_2$  requires C, 52.7; H, 3.7; N, 4.4%):  $\tilde{\nu}_{max}/cm^{-1}(CO)$  1667s, 1641vs and 1601m; (NH) 3463m, 3349m and 3159w  $cm^{-1}$ ;  $\delta_H(CDCl_3)$  7.6–7.1 (30 H, m, Ph) and 5.45 (2 H, s, NH<sub>2</sub>);  $[(CD_3)_2SO]$  10.68 (1 H, s, NH), 7.9–7.1 (30 H, m, Ph) and 5.91 (2 H, s, NH<sub>2</sub>);  $m/z$  888 ( $M^+$ ).

*Method 2.* The complex  $[Pt(PPh_3)_2(CO_3)]$  (0.150 g, 0.19 mmol) was dissolved in  $CH_2Cl_2$  (50 cm<sup>3</sup>) and  $H_4L$  (0.100 g, 0.58 mmol) added. The mixture was stirred for 20 h after which the



Scheme 2 (i) KCl; (ii) CH<sub>2</sub>Cl<sub>2</sub>, reflux; (iii) *cis*-[PtCl<sub>2</sub>(PPh<sub>3</sub>)<sub>2</sub>], Ag<sub>2</sub>O, thf, reflux

solution was filtered, the volume of solvent reduced under reduced pressure, and hexane added to give a mixture of **1** and **2**, as identified by IR and <sup>31</sup>P-<sup>1</sup>H NMR spectroscopy.

[Pt(dppe)(H<sub>2</sub>L)] **3**. The compound dppe (0.160 g, 0.40 mmol) was added to a solution of [Pt(cod)Cl<sub>2</sub>] (0.150 g, 0.40 mmol) in dichloromethane (30 cm<sup>3</sup>) to give a colourless solution of [PtCl<sub>2</sub>(dppe)]; H<sub>4</sub>L (0.225 g, 1.31 mmol) and silver(i) oxide (0.400 g, 1.73 mmol) were then added and the mixture was refluxed for 24 h. The resulting yellow solution was filtered to remove unreacted H<sub>4</sub>L and Ag<sub>2</sub>O and the solvent was removed under reduced pressure. The crude product was recrystallised from dichloromethane-hexane to give yellow crystals of complex **3** (Found: C, 43.5; H, 3.6; N, 5.5. C<sub>31</sub>H<sub>27</sub>N<sub>3</sub>O<sub>4</sub>P<sub>2</sub>Pt·0.25CH<sub>2</sub>Cl<sub>2</sub> requires C, 43.3; H, 3.6; N, 5.5%).  $\tilde{\nu}_{\max}/\text{cm}^{-1}$  (CO) 1677s, 1618s and 1590m; (NH) 3451s, 3356m and 3133w;  $\delta_{\text{H}}(\text{CDCl}_3)$  7.9–7.4 (20 H, m, Ph), 5.55 [2 H, s (br), NH<sub>2</sub>] and 2.20 (4 H, m, CH<sub>2</sub>); [(CD<sub>3</sub>)<sub>2</sub>SO] 10.23 (1 H, s, NH), 7.7–7.0 (20 H, m, Ph), 5.19 (2 H, s, NH<sub>2</sub>) and 2.0 (4 H, m, CH<sub>2</sub>); *m/z* 762 (*M*<sup>+</sup>).

[Pd(dppe)(H<sub>2</sub>L)] **4**. Orange crystals of complex **4** were prepared from [Pd(cod)Cl<sub>2</sub>] (0.200 g, 0.70 mmol), dppe (0.279 g, 0.70 mmol), H<sub>4</sub>L (0.340 g, 1.99 mmol) and silver(i) oxide (0.430 g, 1.86 mmol) in a procedure identical to that for **3** (Found: C, 53.7; H, 4.2; N, 5.8. C<sub>31</sub>H<sub>27</sub>N<sub>3</sub>O<sub>4</sub>P<sub>2</sub>Pd·0.25CH<sub>2</sub>Cl<sub>2</sub> requires C, 54.0; H, 4.0; N, 6.0%).  $\tilde{\nu}_{\max}/\text{cm}^{-1}$  (CO) 1672m, 1617s and 1587m; (NH) 3451m, 3340m and 3119w;  $\delta_{\text{H}}(\text{CDCl}_3)$  7.9–7.3 (20 H, m, Ph), 5.49 [2 H, s (br), NH<sub>2</sub>] and 2.32 (4 H, m, CH<sub>2</sub>); (CD<sub>3</sub>)<sub>2</sub>SO 10.02 (1 H, s, NH), 7.8–7.5 (20 H, m, Ph), 5.11 (2 H, s, NH<sub>2</sub>) and 2.3 (4 H, m, CH<sub>2</sub>); *m/z* 673 (*M*<sup>+</sup>).

[Pt<sub>2</sub>(PPh<sub>3</sub>)<sub>4</sub>(HL)]BF<sub>4</sub> **5**<sup>+</sup>BF<sub>4</sub><sup>-</sup>. Complex **2** (0.150 g, 0.17 mmol) was dissolved in CH<sub>2</sub>Cl<sub>2</sub> (20 cm<sup>3</sup>) and a solution of NaBF<sub>4</sub> (0.500 g, 4.55 mmol) in water (20 cm<sup>3</sup>) was added. The two-layer mixture was stirred vigorously for 10 h and allowed to stand for 2 h. The yellow CH<sub>2</sub>Cl<sub>2</sub> layer was separated, and the solvent removed under reduced pressure. The crude solid was dried and then recrystallised from dichloromethane-hexane to give yellow crystals of **5**<sup>+</sup>BF<sub>4</sub><sup>-</sup>. Yield 0.127 g (94%) (Found: C, 54.2; H, 3.9; N, 2.4. C<sub>77</sub>H<sub>62</sub>BF<sub>4</sub>N<sub>3</sub>O<sub>4</sub>P<sub>4</sub>Pt<sub>2</sub> requires C, 54.6; H, 3.7; N, 2.5%).  $\tilde{\nu}_{\max}/\text{cm}^{-1}$  (CO) 1665s and 1594s; (NH) 3457m, 3318m and 3119m; (BF<sub>4</sub>) 1087vs;  $\delta_{\text{P}}(\text{CDCl}_3)$  -4054 [dd, <sup>1</sup>J(PPt) 4050, 3027] and -4143 [dd, <sup>1</sup>J(PPt) 3893, 3399 Hz];  $\delta_{\text{H}}(\text{CDCl}_3)$  8.0 [1 H, s (br), NH], 7.9–7.4 (60 H, m, Ph) and 5.1 [1 H, t, <sup>2</sup>J(HPt) 67, <sup>3</sup>J(HPt) 5 Hz, PtNH]; *m/z* 1607 (*M* + H<sup>+</sup>) and 1694 (*M* + BF<sub>4</sub><sup>-</sup>).

The above reaction was repeated using complex **1** instead of **2** and the product identified spectroscopically as **5**<sup>+</sup>BF<sub>4</sub><sup>-</sup>.

Reaction of **2** with NaBF<sub>4</sub> (in thf-water and in dichloromethane only), KBF<sub>4</sub>, KPF<sub>6</sub>, LiNO<sub>3</sub>, RbNO<sub>3</sub>, CsNO<sub>3</sub>, Zn(NO<sub>3</sub>)<sub>2</sub> (all in dichloromethane-water) and NaBPh<sub>4</sub> (in dichloromethane-ethanol) also led to **5**<sup>+</sup>X<sup>-</sup> as the only product whereas NBu<sub>4</sub>PF<sub>6</sub> (in dichloromethane) gave no reaction.

[Pt<sub>2</sub>(PPh<sub>3</sub>)<sub>4</sub>(HL)]Cl, **5**<sup>+</sup>Cl<sup>-</sup>. *Method 1*. Complex **1** (0.100 g, 0.11 mmol) was dissolved in dichloromethane (40 cm<sup>3</sup>) and the solution refluxed for 6 h. The resulting solution was cooled, the volume of solvent reduced to 10 cm<sup>3</sup> under reduced pressure, and hexane added to give yellow microcrystals of **5**<sup>+</sup>Cl<sup>-</sup> (Found: C, 52.9; H, 3.5; N, 2.4. C<sub>77</sub>H<sub>62</sub>ClN<sub>3</sub>O<sub>4</sub>P<sub>4</sub>Pt<sub>2</sub>·1.5CH<sub>2</sub>Cl<sub>2</sub> requires C, 53.3; H, 3.7; N, 2.4%).  $\tilde{\nu}_{\max}/\text{cm}^{-1}$  (CO) 1658m, 1627m, 1593s and 1582s; (NH) 3405s and 3321m;  $\delta_{\text{H}}(\text{CDCl}_3)$  7.9–7.3 (60 H, m, Ph) and 5.5 (1 H, m, PtNH).

*Method 2*. Complex **2** (0.080 g, 0.090 mmol) was dissolved in CH<sub>2</sub>Cl<sub>2</sub> (20 cm<sup>3</sup>) and a solution of KCl (0.100 g, 1.34 mmol) in water (20 cm<sup>3</sup>) added. The two-layer mixture was stirred vigorously for 10 h and allowed to stand for 2 h. The yellow CH<sub>2</sub>Cl<sub>2</sub> layer was separated, and the solvent removed under reduced pressure. The crude solid was dried and then recrystallised from dichloromethane-hexane to give yellow crystals of **5**<sup>+</sup>Cl<sup>-</sup> which were identified on the basis of IR and <sup>31</sup>P-<sup>1</sup>H NMR spectroscopy.

*Method 3*. Triphenylphosphine (0.060 mg, 0.23 mmol) was added to a solution of [Pt(cod)Cl<sub>2</sub>] (0.043 g, 0.11 mmol) in thf (30 cm<sup>3</sup>), and the resulting solution of *cis*-[PtCl<sub>2</sub>(PPh<sub>3</sub>)<sub>2</sub>] was added to a solution of complex **1** (0.100 g, 0.11 mmol), also in thf (30 cm<sup>3</sup>). Silver(i) oxide (0.120 g, 0.52 mmol) was then added, and the mixture refluxed for 5 h. The volume of the solvent was reduced by half under reduced pressure and the solution filtered. The yellow solid was abstracted from unreacted Ag<sub>2</sub>O with dichloromethane, and its identity as **5**<sup>+</sup>Cl<sup>-</sup> was confirmed on the basis of IR and <sup>31</sup>P-<sup>1</sup>H NMR spectroscopy.

### Crystallography

A summary of the crystal data, data-collection and structure-solution and refinement parameters for complexes **1**, **2** and **5**<sup>+</sup>BF<sub>4</sub><sup>-</sup> is given in Table 5. The structures were solved by the heavy-atom method, and all the non-hydrogen atoms of the complexes were refined anisotropically, with the phenyl rings being treated as optimised rigid bodies. In **1** a Δ*F* map revealed the presence of 2.5 chloroform molecules (disordered over five partial-occupancy sites) and a single, 25%-occupancy dichloromethane molecule; the major-occupancy chlorine atoms of these molecules were refined anisotropically. In **2** a single, 50%-

**Table 5** Crystallographic data for complexes **1**, **2** and  $5^+BF_4^-$ <sup>a</sup>

	<b>1</b>	<b>2</b>	$5^+BF_4^-$
Empirical formula	C <sub>41</sub> H <sub>33</sub> N <sub>3</sub> O <sub>4</sub> P <sub>2</sub> Pt	C <sub>41</sub> H <sub>33</sub> N <sub>3</sub> O <sub>4</sub> P <sub>2</sub> Pt	[C <sub>77</sub> H <sub>62</sub> N <sub>3</sub> O <sub>4</sub> P <sub>4</sub> Pt <sub>2</sub> ][BF <sub>4</sub> ]
Solvent	1.25CHCl <sub>3</sub> ·0.125CH <sub>2</sub> Cl <sub>2</sub>	0.5 CH <sub>2</sub> Cl <sub>2</sub>	CH <sub>2</sub> Cl <sub>2</sub> ·H <sub>2</sub> O
<i>M</i>	1048.6	931.2	1797.1
Colour, habit	Yellow plates	Yellow octahedra	Yellow needles
Crystal size/mm	0.43 × 0.40 × 0.10	0.67 × 0.67 × 0.33	0.50 × 0.13 × 0.13
Crystal system	Monoclinic	Tetragonal	Triclinic
Space group	<i>P</i> 2 <sub>1</sub> / <i>n</i>	<i>I</i> 4 <sub>1</sub> / <i>a</i>	<i>P</i> $\bar{1}$
<i>a</i> /Å	15.665(3)	23.412(2)	9.692(2)
<i>b</i> /Å	24.009(4)	—	21.100(3)
<i>c</i> /Å	28.146(6)	33.004(6)	22.196(3)
$\alpha$ /°	—	—	116.92(1)
$\beta$ /°	104.66(2)	—	96.05(2)
$\gamma$ /°	—	—	92.84(1)
<i>U</i> /Å <sup>3</sup>	10 241(3)	18 089(5)	4000(1)
<i>Z</i>	8 <sup>b</sup>	16	2
<i>D</i> <sub>c</sub> /g cm <sup>-3</sup>	1.360	1.368	1.492
$\mu$ /mm <sup>-1</sup>	3.049	3.271	3.698
<i>F</i> (000)	4142	7376	1772
2 $\theta$ Range/°	7–45	7–45	4–50
Independent reflections	13 250	5876	13 353
Observed reflections [ $ F_o  > 4\sigma( F_o )$ ]	5906	3767	7432
Absorption correction	Semi-empirical	Empirical	Semi-empirical
Maximum, minimum transmission	0.1817, 0.1102	0.7852, 0.2936	0.6146, 0.4989
Number of parameters	924	424	758
Refinement based on	<i>F</i>	<i>F</i> <sup>2</sup>	<i>F</i> <sup>2</sup>
<i>g</i> in weighting scheme <sup>c</sup>	0.0007	0.0007	0.067, 0.622 <sup>d</sup>
Final <i>R</i> ( <i>R'</i> ) <sup>e</sup>	0.051 (0.050)	0.037 (0.036)	0.061 (0.127 <sup>f</sup> )
Largest and mean $\Delta/\sigma$	0.042, 0.001	0.665, 0.031	−0.156, 0.005
Data/parameter ratio	6.39	8.88	9.80
Largest difference peak, hole/e Å <sup>-3</sup>	1.18, −0.72	0.69, −0.49	0.98, −0.68

<sup>a</sup> Details in common: Siemens P4/PC diffractometer, graphite-monochromated Mo-K $\alpha$  radiation, ( $\lambda = 0.710 73 \text{ \AA}$ ); 293 K;  $\omega$  scans: data corrected for Lorentz-polarisation factors. <sup>b</sup> There are two crystallographically independent molecules in the asymmetric unit. <sup>c</sup>  $w^{-1} = \sigma^2(F_o) + gF_o^2$ . <sup>d</sup> Values given are for *a* and *b* in  $w^{-1} = \sigma^2(F_o^2) + (aP)^2 + bP$ . <sup>e</sup>  $R = \Sigma||F_o| - |F_c||/\Sigma|F_o|$ . <sup>f</sup> Value given is for  $wR2 = [\Sigma w(F_o^2 - F_c^2)^2/\Sigma w(F_o^2)^2]$ <sup>g</sup>.

occupancy, dichloromethane molecule was located, the chlorine atoms of which were refined anisotropically. The structure of  $5^+BF_4^-$  was found to contain a dichloromethane and a water molecule, disordered over four and two partial-occupancy sites respectively; these molecules were refined isotropically.

For **2** the N–H hydrogen atoms were located from a  $\Delta F$  map and refined isotropically subject to an N–H distance constraint (0.90 Å). All the other hydrogen atoms in the three structures were placed in calculated positions, assigned isotropic thermal parameters,  $U(H) = 1.2U_{eq}(C/N)$ , and allowed to ride on their parent atoms. In  $5^+BF_4^-$  the hydrogen atoms of the disordered water molecule could not be located.

Computations were carried out on 50 MHz 486 personal computers using the SHELXTL PC program system.<sup>23</sup>

Atomic coordinates, thermal parameters, and bond lengths and angles have been deposited at the Cambridge Crystallographic Data Centre (CCDC). See Instructions for Authors, *J. Chem. Soc., Dalton Trans.*, 1996, Issue 1. Any request to the CCDC for this material should quote the full literature citation and the reference number 186/182.

## Acknowledgements

The EPSRC is thanked for financial support and BP plc is thanked for endowing D. M. P. M.'s chair.

## References

- 1 A. D. Burrows, C.-W. Chan, M. M. Chowdhry, J. E. McGrady and D. M. P. Mingos, *Chem. Soc. Rev.*, 1995, **24**, 329.
- 2 S. Subramanian and M. J. Zaworotko, *Coord. Chem. Rev.*, 1994, **137**, 357.
- 3 G. M. Whitesides, E. E. Simanek, J. P. Mathias, C. T. Seto, D. N.

- Chin, M. Mammen and D. M. Gordon, *Acc. Chem. Res.*, 1995, **28**, 37.
- 4 J. A. Zerkowski and G. M. Whitesides, *J. Am. Chem. Soc.*, 1994, **116**, 4298.
- 5 J.-M. Lehn, M. Mascal, A. DeCian and J. Fischer, *J. Chem. Soc., Perkin Trans. 2*, 1992, 461.
- 6 A. D. Burrows, D. M. P. Mingos, A. J. P. White and D. J. Williams, *J. Chem. Soc., Dalton Trans.*, 1996, 149.
- 7 W. I. Sundquist and S. J. Lippard, *Coord. Chem. Rev.*, 1990, **100**, 293.
- 8 B. Lippert, *Prog. Inorg. Chem.*, 1989, **37**, 1.
- 9 W. M. Beck, J. C. Calabrese and N. D. Kottmair, *Inorg. Chem.*, 1979, **18**, 176.
- 10 B. Roy, A. K. Singh and R. P. Singh, *Talanta*, 1983, **30**, 617.
- 11 D. Lalart, G. Dodin and J.-E. Dubois, *J. Chim. Phys.*, 1982, **79**, 449.
- 12 S. P. Perlepes, V. Lazaridou, B. Sankhla and J. M. Tsangaris, *Bull. Soc. Chim. Fr.*, 1990, **127**, 597.
- 13 D. Sen and W. Gilbert, *Nature (London)*, 1988, **334**, 364.
- 14 G. Laughlan, A. I. H. Murchie, D. G. Norman, M. H. Moore, P. C. E. Moody, D. M. J. Lilley and B. Luisi, *Science*, 1994, **265**, 520.
- 15 J. R. Williamson, M. K. Raghuraman and T. R. Cech, *Cell*, 1989, **59**, 871.
- 16 D. S. Lawrence, T. Jiang and M. Levett, *Chem. Rev.*, 1995, **95**, 2229.
- 17 H. Rauter, E. C. Hillgeris, A. Erxleben and B. Lippert, *J. Am. Chem. Soc.*, 1994, **116**, 616.
- 18 P. J. Stang, D. H. Cao, S. Saito and A. M. Arif, *J. Am. Chem. Soc.*, 1995, **117**, 6273.
- 19 F. D. Rochon, A. Morneau and R. Melanson, *Inorg. Chem.*, 1988, **27**, 10.
- 20 D. Drew and J. R. Doyle, *Inorg. Synth.*, 1972, **13**, 48.
- 21 J. Chatt, L. M. Vallarino and L. M. Venanzi, *J. Chem. Soc.*, 1957, 3413.
- 22 D. M. Blake and D. M. Roundhill, *Inorg. Synth.*, 1978, **18**, 120.
- 23 SHELXTL PC, versions 4.2 and 5.03, Siemens Analytical X-Ray Instruments, Madison, WI, 1990 and 1994.

Received 22nd May 1996; Paper 6/03585J